

杨容, 杨西燕, 范存辉, 等. 川东地区中二叠统茅口组岩溶储层特征及其主控因素[J]. 中国岩溶, 2025, 44(2): 419-433.

DOI: [10.11932/karst20250216](https://doi.org/10.11932/karst20250216)

川东地区中二叠统茅口组岩溶储层特征及其主控因素

杨容¹, 杨西燕¹, 范存辉¹, 李阳¹, 李玥², 黄梓桑³

(1. 西南石油大学地球科学与技术学院, 四川成都 610500; 2. 中国石油西南油气田公司勘探开发研究院, 四川成都 610041; 3. 成都理工大学, 四川成都 610059)

摘要: 川东地区中二叠统茅口组普遍发育岩溶储层。基于大量野外露头、钻井岩心、薄片、测井、录井解释资料以及地震资料, 对岩溶储层特征及主控因素进行综合分析。研究结果表明: (1) 岩溶储层具有多种识别标志, 岩心与露头上, 常具有残余溶蚀孔洞与裂缝, 地层顶部可见铝土质黏土岩及含褐铁矿的岩溶角砾; 测井上, 声波时差、补偿中子、补偿密度曲线与双侧向电阻率曲线均呈现箱型、成像测井表现为黑色斑块状; 录井上, 见井漏与放空; 地震剖面上, 呈现出“低频、强振幅、宽波峰”特征, 当缝洞较多时还会出现“亮点”反射特征。(2) 岩溶储层的储集岩主要为颗粒灰岩, 储集空间主要为溶孔、溶洞; 储层物性表现为低孔低渗的特征, 孔洞型储层物性最佳; 纵向上, 岩溶储层主要分布在距茅口组顶部 100 m 范围内, 孔洞型储层最为发育; 横向分布延展性较差; 平面上在邻水—丰都一带呈北西—南东向的带状分布。(3) 颗粒滩为岩溶储层优质的物质基础, 并为后期成岩流体提供渗滤通道; 岩溶古地貌控制了岩溶储层分布, 高产井多分布于岩溶陡坡与岩溶缓坡的残丘地貌单元中, 岩溶高地与岩溶陡坡的过渡区也是岩溶储层发育的有利区; 多期裂缝改善了储层的储集性能, 并为油气渗滤提供通道, 促进大型油气藏的聚集。故建议将茅口组中上部颗粒滩与裂缝发育的残丘地区作为下步油气勘探开发重点区。

关键词: 岩溶储层; 储层特征; 主控因素; 茅口组; 川东地区

创新点: 融合岩石学、测井、录井及地震等资料, 系统建立岩溶储层识别响应特征; 明确其纵横向及平面优势发育带, 提出“颗粒滩奠基—古地貌控储—裂缝增效”三种控制因素, 预测邻水—丰都及达州—开江岩溶残丘新靶区, 研究成果为深层岩溶油气勘探提供新思路。

中图分类号: P618.13 文献标识码: A

文章编号: 1001—4810 (2025) 02—0419—15

开放科学(资源服务)标识码(OSID):



0 引言

虽然碳酸盐岩分布面积仅占全球沉积岩总面积的 20%, 但其蕴藏的油气资源占世界总储量的 52%^[1], 可见碳酸盐岩储层对于油气勘探与开发具有至关重要的意义^[2]。岩溶储层作为碳酸盐岩储层的重要类型之一, 因其分布强烈非均质性, 导致优质

岩溶储层的预测仍是碳酸盐油气储层勘探的一大难点^[3]。目前常用的岩溶储层预测方法主要有地质方法和地球物理方法^[4]。而地球物理模型与各种参数又多基于地质方法实现。因此, 从地质学角度, 系统构建岩溶储层识别标志, 明确储层分布特征, 厘清其主控因素, 在优质岩溶储层的预测及油气勘探开发中至关重要。

资助项目: 中国石油天然气股份有限公司油气和新能源分公司科学与技术开发项目(2022KT0401)

第一作者简介: 杨容(2001—), 女, 在读硕士研究生, 研究方向为沉积学与储层地质学。E-mail: 1756900190@qq.com。

通信作者: 杨西燕(1982—), 女, 博士, 副教授, 研究方向为沉积学与储层地质学。E-mail: zz-yxy1982@sina.com。

收稿日期: 2024—07—16

受东吴运动影响,四川盆地整体抬升,导致茅口组大规模发育岩溶储层^[5]。由于在岩溶储层中油气勘探持续突破,前人对于其识别、分布及主控因素进行了大量研究^[6-12]。针对茅口组岩溶储层识别标志,由以往通过单一的岩心、钻井、测井、录井与地震资料进行识别,发展到如今利用井-震结合的方式识别,增加了岩溶储层识别的准确性。江青春等^[6]认为茅口组岩溶储层的识别特征为岩心上具有溶蚀孔洞,测井呈现自然伽马高值,有放空与漏失等录井显示,地震资料上反射信号杂乱、振幅弱、亮点明显;李素华等^[7]识别出优质生屑滩岩溶储层呈北西向分布于元坝地区缓坡破折带上。此外,岩溶储层与古风化壳有关,戴晓峰等^[8]通过统计发现川中茅口组的岩溶储层主要分布在距离其顶界的100 m范围内;冯磊等^[9]在研究泸州地区茅口组岩溶储层时指出,在岩溶斜坡中发育更多优质岩溶储层。岩溶储层发育的主控因素较为复杂;杨铭磊等^[10]认为川南地区早期岩溶储层的形成以相控为主;而王国锋等^[11]则认为自贡地区缝洞型岩溶储层的形成是沉积相、古地貌与断裂带共同控制的结果;曹华等^[12]认为川东地区缝洞型岩溶储层的形成,不仅受到了古地貌的控制,还有东吴运动、火山活动与古气候的综合影响。

尽管许多学者在这方面已取得显著的研究成果,但尚未系统分析茅口组岩溶储层识别标志与储层特征及主要控制因素。本文以川东地区茅口组岩溶储层为研究对象,基于大量野外露头、钻井岩心、薄片、测井、录井以及地震资料,形成一套岩溶储层识别方法,结合岩溶储层发育特征,综合分析其控制因素,以期为岩溶储层的预测提供新依据。

1 区域地质概况

研究区位于四川盆地广安以东,巫山以西,城口以南,重庆以北,地处于四川省中东部和重庆市东北部;构造位置处于上扬子板块东北缘的川东高陡构造带、大巴山断褶带、川湘断褶带的过渡区^[13](图1a)。上扬子中、晚二叠世的东吴运动与峨眉地幔柱上涌引发的地壳快速差异抬升^[14],使四川盆地在茅口组沉积中晚期发生构造-沉积分异,同时导致茅口组顶部遭受1~3 Ma的暴露,产生不同程度的剥蚀,形成了茅口组顶部的岩溶储层^[15-16]。

研究区茅口期沉积早期(茅一段—茅二c亚段)海侵期能量较低,处于碳酸盐岩缓坡相,仅存在少量低能颗粒滩,主要沉积灰黑色(含)生屑泥晶灰岩与泥质灰岩,泥质含量较高,眼球一眼皮构造发育^[17];中晚期(茅二b—茅三段)受东吴运动影响发生沉积分异,呈现隆凹相间的沉积格局,在水体能量相对较强的海退高水位体系域中大规模台内滩继承性发育^[18],研究区逐步过渡为碳酸盐岩台地相,发育厚层块状的生屑灰岩与泥晶灰岩,生物化石含量丰富,种类繁多;晚期由于东吴运动持续影响与峨眉地幔柱上涌,使盆地地层进一步抬升并产生差异性沉降,在川北—川东北部地区形成裂陷槽锥形,形成茅口组末期的台地相、海槽相差异沉积,在台地相中沉积的茅四段主要为中—厚层深灰色泥晶灰岩和灰黑色含泥质灰岩,有机质含量较高,而海槽相中沉积的孤峰段则以薄层黑—灰黑色泥页岩、硅质泥岩为主,泥质含量高^[19-20](图1b,图1c)。

研究区茅口组残余厚度总体分布在120~340 m范围内。整体呈“两薄夹一厚”的分布特征,南高北低,东高西低(图2)。地层厚度高值区集中在邻水—丰都一带。

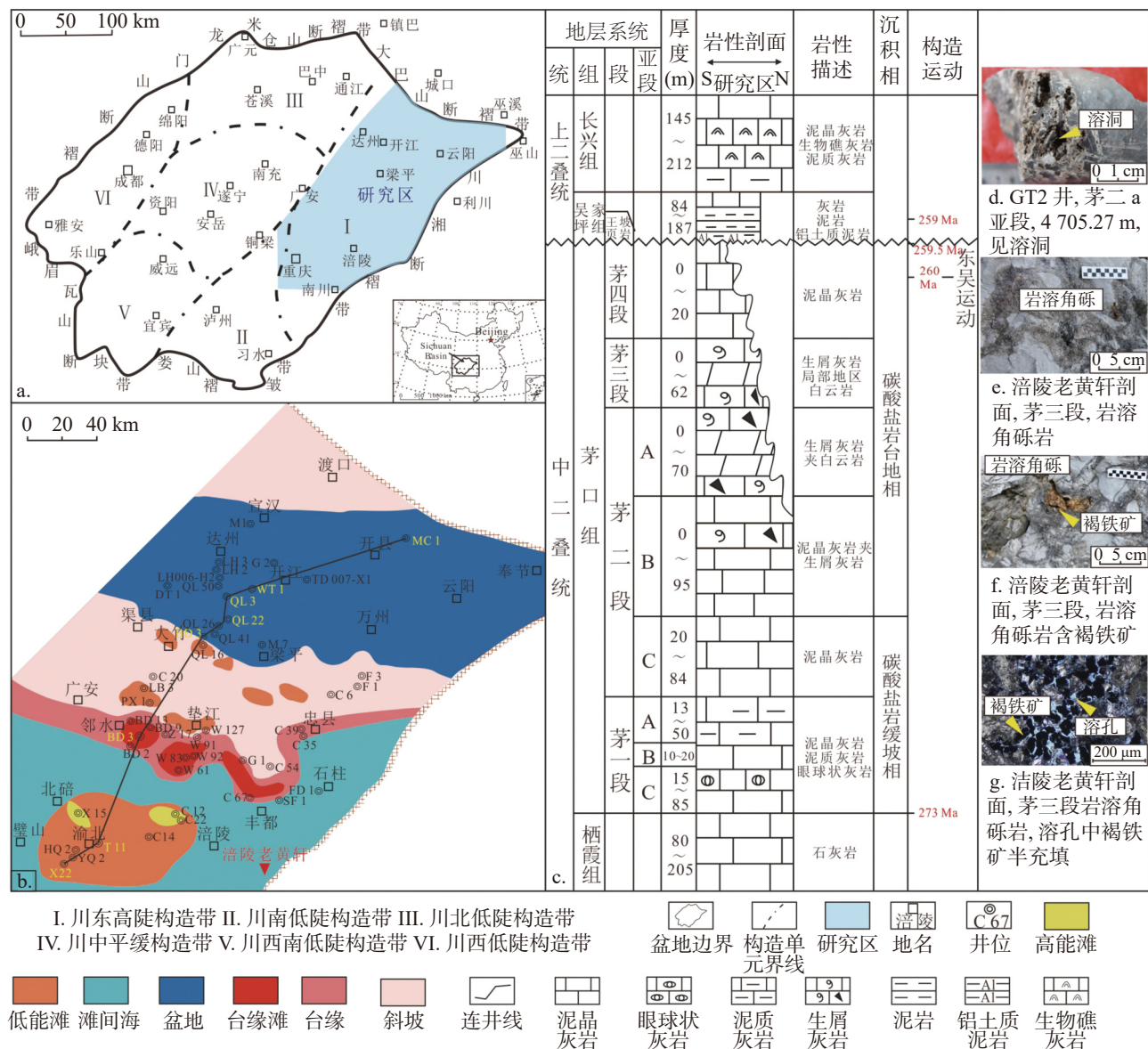
2 岩溶储层响应特征

2.1 岩石学响应特征

研究区中二叠统茅口组岩溶储层表现出特定的岩石学特征,其成因主要为:一方面由于东吴运动的影响,导致茅口组顶部长期遭受大气淡水的溶蚀,沿着先期孔隙与裂缝形成岩溶孔洞缝(图1d);另一方面接近地表的地层遭受风化作用,在侵蚀面上形成风化壳,形成铝土质黏土岩及岩溶垮塌作用形成的岩溶角砾(图1e),且岩溶角砾中充填着次生矿物褐铁矿^[21](图1f,图1g)。

2.2 测井响应特征

岩溶作用形成特殊岩溶缝洞型储层在测井曲线上具有不同的响应特征,其中声波时差、补偿中子、补偿密度曲线(合称“三孔隙度曲线”)与深浅双侧向电阻率曲线变化特征最为明显(图3)。在岩溶孔洞型储层发育段,由于其放射性元素含量较低或受到屏蔽效应的影响^[22],自然伽玛数值通常小于40API;三孔隙度曲线具有较好的一致性,整体呈现箱型,补



a. 四川盆地构造分带图 b. 川东地区茅二 a 亚段沉积相图(据文献[19]改) c. 川东地区茅口组地层柱状图 d-g. 茅口组岩溶储层岩石学识别特征图

Fig. 1 Regional geological overview of the study area

a. Structural zoning map of the Sichuan Basin b. Sedimentary facies map of the Maojia sub section in the eastern Sichuan region (revised according to reference [19]) c. Stratigraphic column chart of the Maokou Formation in the eastern Sichuan region d-g. Petrographic identification characteristics map of the Maokou Formation karst reservoir

偿中子与声波时差值均小幅增大,补偿密度具有明显的降低趋势;双侧向电阻率值呈箱型或漏斗型正差异降低。且溶蚀孔洞在成像测井上表现为低阻高导的黑色斑块状,其周围具有逐渐过渡到黄色的浸染特征。在较大溶洞时段,声波时差曲线会出现跳波现象,井径会明显增大。

在裂缝型储层发育时段,一般溶蚀孔、洞不发育,孔隙度一般低于1%,但渗透率较高,三孔隙度曲线相关性较差,裂缝发育位置声波时差曲线值增大。

当存在低角度裂缝时,声波时差曲线具有大幅跳跃特征,补偿密度与补偿中子曲线无响应或小幅度降低;深浅双侧向电阻率值差异不大,表现为负差异降低,而高角度裂缝表现为正差异降低。

岩溶缝洞型储层发育时段,测井曲线锯齿状特征明显,自然伽玛值较低、三孔隙度曲线呈现锯齿状跳波而与孔洞型储层相区分,补偿中子与声波时差值均增大,补偿密度值降低;深浅双侧向电阻率值相差较大,通常呈正差异降低特征。

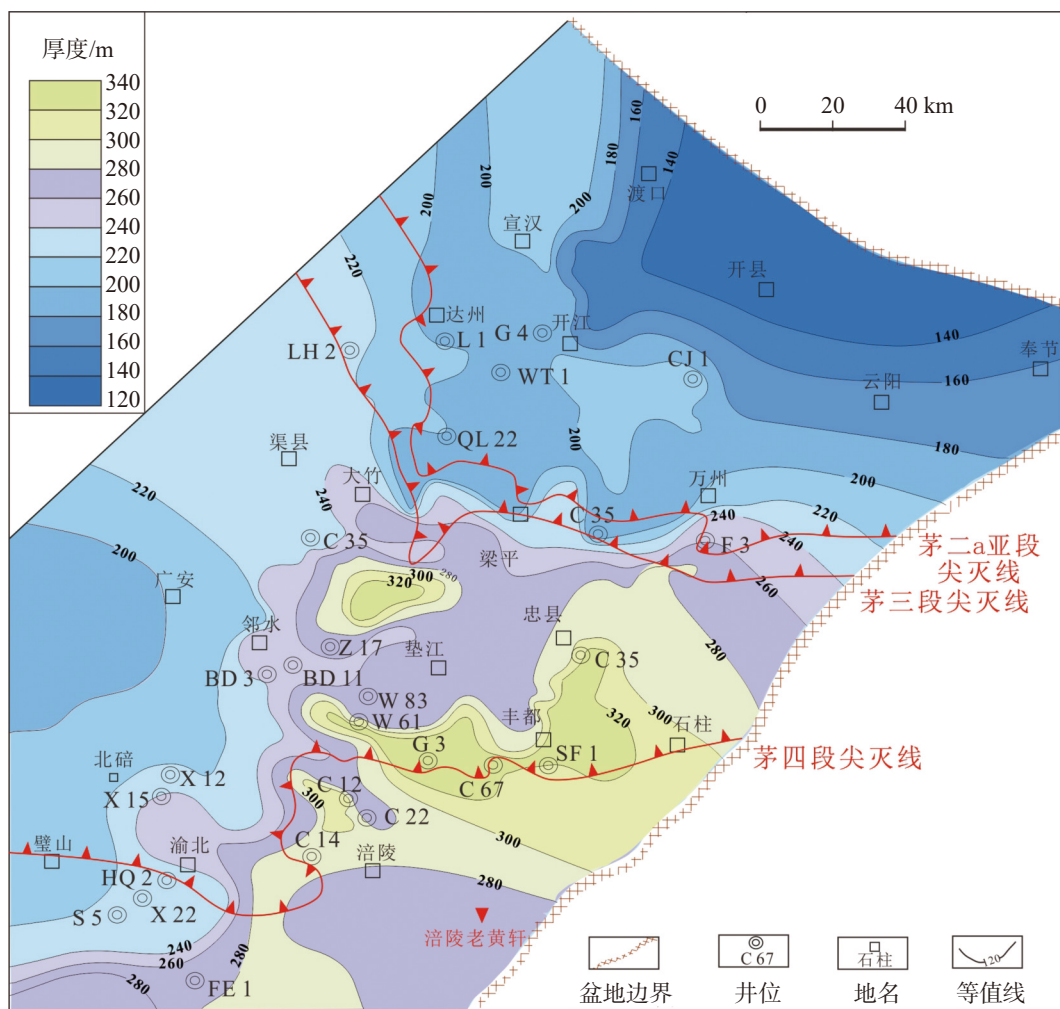


图2 川东地区中二叠统茅口组地层残余厚度等值线图

Fig. 2 Isoline map of residual thickness of the Middle Permian Maokou Formation in the eastern Sichuan basin

2.3 录井响应特征

在钻井过程中,若所钻地层存在自然的漏失通道,如高渗透地层、裂隙性地层和溶洞性地层往往会发生井漏、井涌、放空等录井显示。而岩溶作用对碳酸盐岩溶蚀起到明显促进作用,可使其产生大量溶蚀孔洞^[23]。因此井漏、井涌、放空、气侵与气测异常等录井显示也可以表现出岩溶储层的发育程度。井漏主要发生在距茅口组顶部以下0~50 m范围内,其次为其下50~100 m范围内(图4),集中发生在茅二段与茅三段(图5)。放空与井涌在茅口组各段均有发育,但总体也主要在茅二段与茅三段。钻遇茅二段与茅三段气显示井位较多(图5)。如龙会场LH2井直眼钻进茅二段井喷失控,测试产量 $206.46 \times 10^4 \text{ m}^3 \cdot \text{d}^{-1}$;侧钻时茅二段放空0.4 m,并发生井漏,共漏失钻井液227.5 m³。这些现象表明研究区茅口组中上部的岩溶缝洞广泛分布,发育有大量的岩溶储层。

2.4 地震响应特征

研究区茅口组顶部大小不一、形态各异的缝洞储渗体主要由构造运动形成的中小断层及伴生的裂隙系统与古岩溶洞穴构成。这些岩溶缝洞储渗体在三维反射剖面上具有明显的响应特征。结合前人的研究发现,岩溶储层在地震上主要表现为“低频、强振幅、宽波峰”的特征^[7,24]。由于地震波穿过茅口组上覆低速介质到达碳酸盐岩高速介质时,波阻抗产生较大的差异而在茅口组顶部产生强反射界面,但当碳酸盐岩中溶洞体发育时,波阻抗差异减小,形成下拉、加宽的异常响应特征,当缝洞较多且杂乱分布时还会出现“杂乱反射、亮点”的特征。由过WT1井的地震剖面(图6)可知,WT1井茅口组顶部共钻遇四套储层,并且出现频繁井漏现象,在地震剖面上也表现为“低频、强振幅、宽波峰”的特征,宽波峰下部呈现“亮点”反射特征,为缝洞发育的表现,而WT

储层类型	声波时差 API	补偿中子 $\mu\text{s}/\text{ft}$	补偿密度 $\text{g}\cdot\text{cm}^{-3}$	深浅侧向 $\Omega\cdot\text{m}$	$\frac{\text{GR}}{200\text{API}}$	$\frac{\text{CAL}}{0 \text{ in } 10}$	曲线形态			岩心照片	成像测井	典型井
							AC 90 $\mu\text{s}/\text{ft}$	40 $2 \Omega\cdot\text{M}$	RLLD CNL DEN RLLS			
孔洞型	45~65 数值增大	0.25~10 数值增大	2.2~2.7 数值减小	100~2 500 数值减小							C54 LB 7	
裂缝型	45~55 数值增大	无响应 无响应	100~1 000 数值减小								QL 50 QL 26 QL 41 W 127 W 61	
缝洞型	46~75 数值增大	0.5~11 数值增大	2.1~2.6 数值减小	100~3 000 数值减小							QL 22 C 67 WT 1	

图3 川东地区茅口组储层类型划分标准图版

Fig. 3 Standard plate of dividing reservoir types in the Maokou Formation in the eastern Sichuan basin

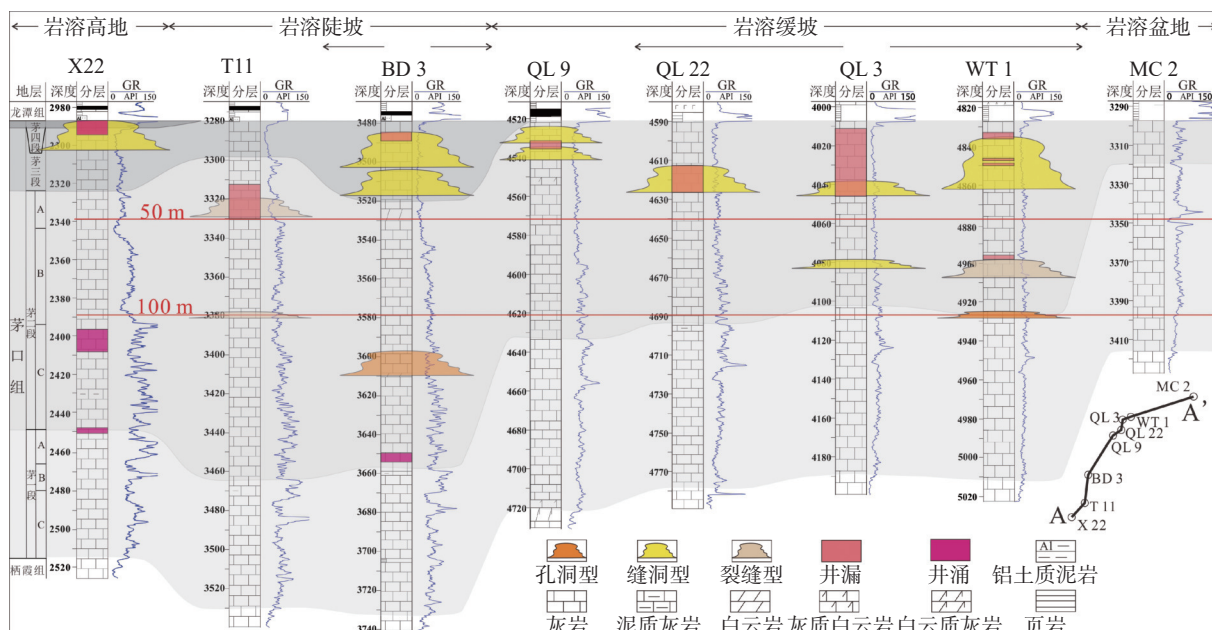


图4 研究区茅口组岩溶储层连井剖面图（剖面位置见图1）

Fig. 4 Cross-well profile diagram of karst reservoirs in the Maokou Formation in the study area (profile location see Figure 1)

1井位置波峰宽度相对左侧有所收缩。

3 岩溶储层特征

3.1 储集岩岩石类型

根据已完钻井取心资料,岩化分析数据、镜下薄

片和测录井资料综合分析,认为研究区岩溶储层储集岩类型主要为颗粒灰岩、含生屑泥晶灰岩、细-中晶白云岩、砂屑灰岩以及白云质(豹斑)灰岩。在各类储集岩中,以颗粒灰岩为主(图7a、b),细-中晶白云岩次之(图7c),其余岩类相对较少。研究区颗粒灰岩主要形成于颗粒滩相中,分布在茅三段与茅

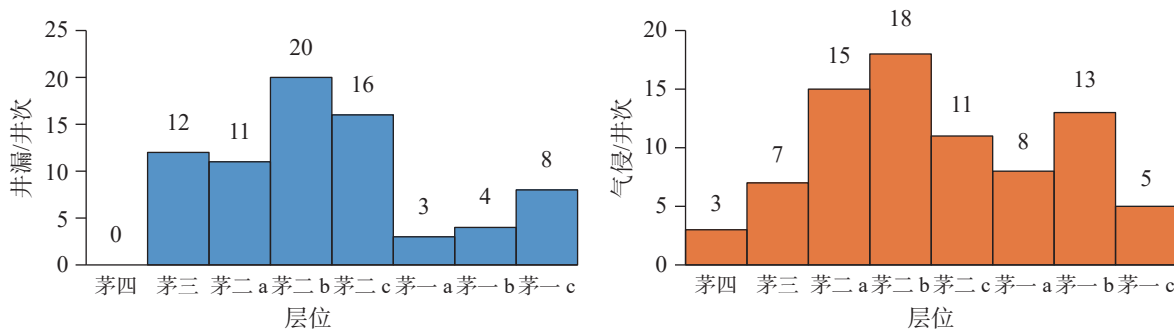


图 5 川东地区茅口组各亚段井漏与气侵分布直方图

Fig. 5 Distribution histogram of well leakage and gas invasion in each sub-member of the Maokou Formation in the eastern Sichuan basin

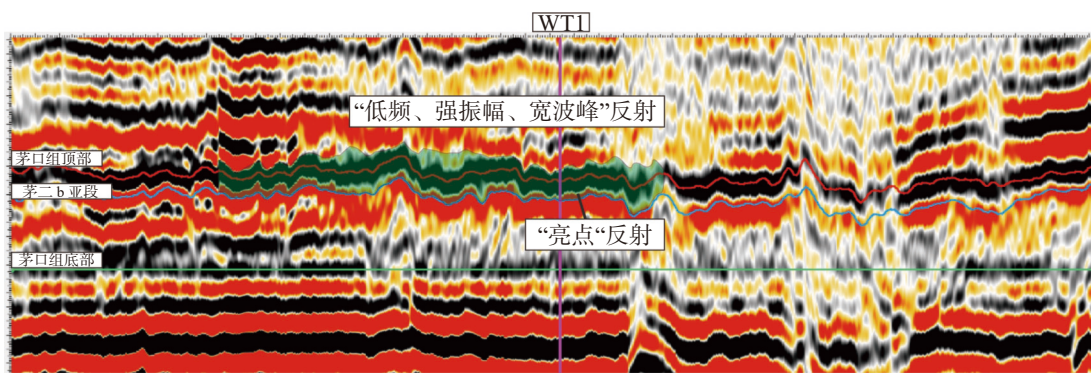


图 6 过 WT 1 井地震剖面图(据文献 [7] 改)

Fig. 6 Seismic profile passing through Well WT 1 (modified according to reference [7])

二段的中上部。颗粒灰岩多呈灰—灰白色，中—厚层块状，磨圆与分选性中等，颗粒含量 50%~70%，生物含量丰富且保存较好，以䗴(Fusulinina)，有孔虫(Foraminifera)、藻类、腕足、苔藓虫与棘皮等生物碎屑为主，其中䗴发育最多，但此类岩石颗粒间常被充填亮晶方解石与泥晶方解石等胶结物而变得致密，后期的岩溶作用的改造可形成良好的储集空间，有利于岩溶储层的形成与保存。

3.2 储集空间类型

研究区茅口组岩溶储层中储集空间主要为：溶孔、溶洞与裂缝。其中溶洞分布最为普遍，多期裂缝对渗滤起到了关键的作用。

研究区内溶孔发育较少，多呈孤立分布，常被方解石、沥青、泥质半—全充填，少部分未被充填(图 7a—图 7d)。粒内溶孔及粒间溶孔主要发育在颗粒灰岩、含生屑泥晶灰岩与砂屑灰岩中。粒内溶孔主要分布在茅二、茅三段中，出现的频率中等，孔隙多呈孤立状分布，连通性较差，颗粒灰岩中被溶蚀的颗粒为生物碎屑和藻屑(图 7b)，若颗粒被完全溶蚀，仅保留原

颗粒外形和大小，则形成铸模孔。粒间溶孔也主要分布在茅二、茅三段，但大多被方解石、白云石或沥青充填(图 7a)。晶间溶孔在研究区岩溶储层中出现频率较低，主要发育在细—中晶白云岩或颗粒灰岩的亮晶胶结物中，通常未充填或被沥青、白云石充填(图 7c)，以 C 67 井最为典型。

溶洞是研究区最重要的储集空间类型，主要发育在颗粒灰岩与细—中晶白云岩中。岩心上呈边缘不规则的圆状、椭圆状或拉长状孔洞顺层或斜交层分布。溶洞之间连通性较差，大小不一，以小洞、中洞为主，直径多数在 2~40 mm，也有部分可达 70 mm，常被方解石、白云石、泥质与沥青半充填，部分未被充填(图 7e, 图 7h)。溶洞性地层是茅口组钻井泥浆漏失频繁的主要原因，尤其是茅二段地层。如 M 1 井发育溶蚀缝洞，未完全充填，在茅二段顶部 0~13 m 内漏失钻井液 1091.0 m³，日产气 1.29×10⁴ m³，日产水 960 m³(图 7j)。

裂缝是流体渗滤的主要通道，也可作为储集空间。当多个裂缝相互连通或与发育的溶蚀孔洞相互沟通时可较好改善储层物性。裂缝依照成因可分为构造缝、压溶缝与溶扩缝；依照期次可分为早期缝、中期

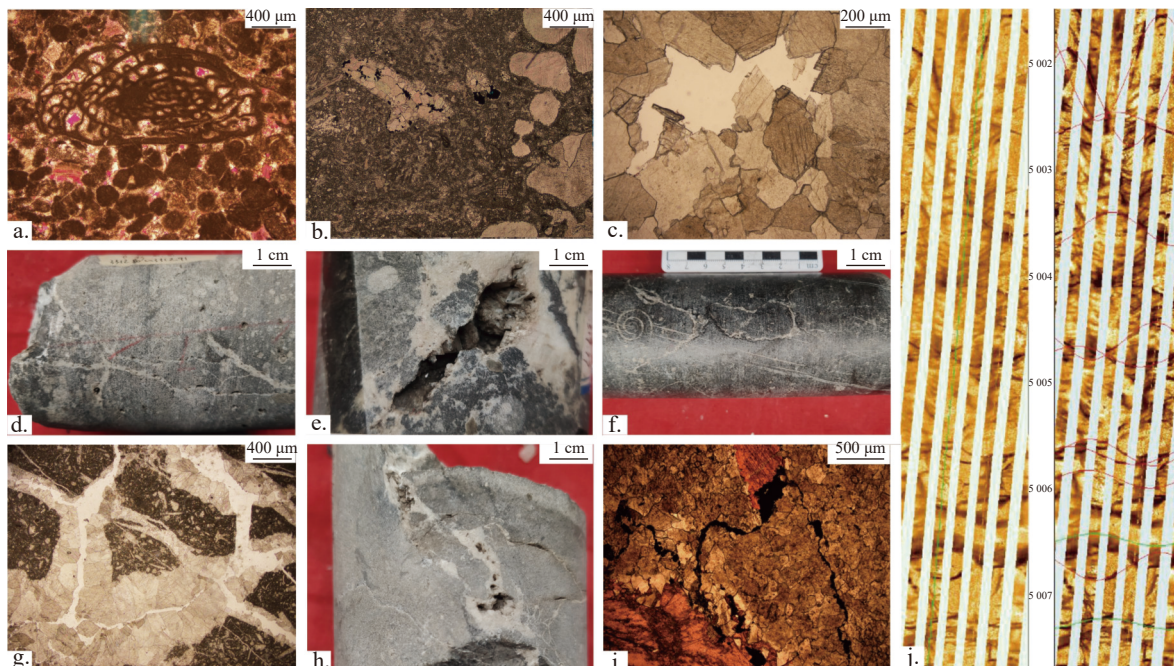


图7 川东茅口组岩溶储层储集空间图版

a. 泥晶生屑灰岩, 粒间孔, C67井, 3276.08~3726.16 m, 茅三段, 正交偏光 b. 生屑灰岩, 粒内溶孔, DT002-4井, 4137.48 m, 茅二b亚段, 单偏光 c. 晶粒白云岩, 晶间溶孔, C67井, 3304.71~3304.76 m, 茅二a亚段, 单偏光 d. 生屑灰岩, 含溶孔溶洞与裂缝, C67井, 3312.80~3312.91 m, 茅二a亚段 e. 生屑灰岩, 长约6 cm溶洞, C67井, 3319.77 m, 茅二a亚段 f. 泥晶灰岩, 裂缝, G2井, 3960.31 m, 茅二b亚段 g. 泥晶生屑灰岩, 溶扩缝, C20井, 3382.46~3382.51 m, 茅二b亚段, 单偏光 h. 亮晶生屑灰岩, 裂缝连通溶洞, C67井, 3314.11 m, 茅口组 i. 亮晶生屑灰岩, 缝合线, C67井, 3321.14~3321.20 m, 茅二a亚段, 单偏光 j. 缝洞型储层段, 井段井漏失量143.0 m³, M1井, 5001.70~2007.90 m, 茅三段

Fig. 7 Plate of karst reservoir storage space in the Maokou Formation in the eastern Sichuan basin

a. Well C67 with intergranular pores in mud crystal bioclastic limestone, 3276.08-3726.16 m, with orthogonal polarization in the Maosan Formation. b. Well DT002-4 with intragranular dissolved pores in the b detrital limestone, 4137.48 m, Mao'er b sub section, single polarized light. c. grain dolomite intergranular dissolution pore C67 well, 3304.71-3304.76 m Mao'er a sub segment single polarization. d. debris ash karst hole+karst cave+crack C67 well, 3312.80-3312.91 m Mao Er a sub section - composite reservoir space. e. Large scale karst cave (6 cm) in E-generated limestone, C67 well, 3319.77 m Mao'er a sub section - significant macroscopic dissolution phenomenon. f. Mud crystal limestone fracture G2 well, 3960.31 m Mao'er b sub section. g. mud crystal debris gray karst expansion crack C20 well, 3382.46-3382.51 m Mao'er b sub segment single polarization dissolution expansion crack. h. The cracks in the H-bright crystal detrital limestone connect to the karst cave C67 well, and the Maokou Formation fracture cave system is developed at a depth of 3314.11 meters. i. The C67 well was formed by the single polarization pressure solution of the Mao'er a sub segment at 3321.14-3321.20 m along the suture line of the i-bright crystal bioclastic limestone. j. Large scale fracture cave system M1 well in J-type reservoir, Maosan section, 5001.70-2007.90m.

缝与晚期缝。研究区以高角度构造缝(中期缝或晚期缝)为主, 约占65%以上(图7f); 溶扩缝(早期缝或中期缝)在研究区也较为常见, 是岩溶水在早期裂缝的基础上经过多期溶蚀扩大后产生的, 可进一步演变成裂缝性溶孔、洞, 通常缝宽可达1~20 mm, 其边缘具有明显溶蚀港湾状(图7g); 压溶缝(早期缝)在研究区中少见, 主要存在于茅口组顶部, 为压溶作用形成的缝合线, 呈锯齿状、波状, 在上覆地层的压力下, 常呈半闭合-闭合状态, 为沥青或泥质等充填(图7i)。

3.3 岩溶储层物性特征

研究区茅口组岩溶储层整体呈现出低孔低渗的物性特征(表1)。其实测孔隙度主要分布范围为

2.0%~8.7%, 平均值为3.4%; 实测渗透率主要分布范围为0.008~65.263 mD, 平均值为18.3 mD。生屑灰岩的孔隙度明显高于其他储集岩, 平均孔隙度为3.7%。它是组成缝洞型与孔洞型储层最重要的储集岩性。研究区以缝洞型岩溶储层物性最佳, 孔隙度平均值为3.3%, 渗透率平均值为23.3 mD。孔洞型储层虽有较高的孔隙度, 但由于缺少渗透通道导致其物性较差。岩溶陡坡平均孔隙度为3.96%, 明显高于岩溶缓坡(平均孔隙度为3.27%)与岩溶高地(平均孔隙度为2.1%)。

3.4 岩溶储层分布特征

研究区茅口组岩溶储层较为发育, 但具显著的

表 1 川东地区茅口组岩溶储层实测物性统计表

Table 1 Statistics of measured physical properties of karst reservoirs in the Maokou Formation in the eastern Sichuan Basin

井名	岩性	层位	孔隙度/%	渗透率/mD	储层类型	岩溶古地貌
QL 15	含生屑泥晶灰岩	茅二b亚段	2.3	0.003		
QL 49	含生屑泥晶灰岩	茅二b亚段	2.0	0.208		
WT 1	生屑灰岩	茅二c亚段	3.9	42.468	裂缝型	
QL 50	砂屑灰岩	茅二b亚段	2.4	0.146		
WT 1	生屑灰岩	茅二b亚段	3.3	25.861		
QL 22	生屑灰岩	茅二b亚段	3.2	48.46		岩溶缓坡
QL 49	生屑灰岩	茅二c亚段	8.7	65.263		
QL 50	生屑灰岩	茅二b亚段	2.1	0.021		
QL 50	生屑灰岩	茅二b亚段	2.3	0.414	缝洞型	
QL 9	含云质灰岩	茅二b亚段	2.5	0.008		
S 6	生屑灰岩	茅二a亚段	2.1	\		岩溶高地
C 62	生屑灰岩	茅三段	3.5	\		
SF 1	生屑灰岩	茅三段	2.4	\		
F 3	生屑灰岩	茅二b亚段	5.9	\		岩溶陡坡
F 3	生屑灰岩	茅二b亚段	5.5	\	孔洞型	
C 62	生屑灰岩	茅四段	2.5	\		

非均质性。从岩溶储层横向连井剖面上可知, 岩溶储层纵向上主要分布在距离茅口组顶部 50 m 范围内, 局部可达 80~100 m, 且缝洞型储层最发育, 层位上主要分布在茅二 a 亚段, 茅三段与茅二 b 亚段也有分布(图 7)。平面上, 茅二 b 亚段岩溶储层厚度在 1~42 m(平均厚度为 9.37 m), 主要沿南北向呈孤立点状分布在开江、达州、万州、渠县以及丰都等地(图 8d); 茅二 a 亚段岩溶储层厚度在 1~29 m(平均厚度为 7.68 m), 呈带状分布在邻北—丰都一带(图 8e); 茅三段岩溶储层厚度在 0.5~23.0 m(平均厚度为 11.04 m), 顺北西—南东向分布在邻水—丰都与大竹—梁平一带(图 8f)。

4 岩溶储层主控因素

4.1 颗粒滩为岩溶储层提供丰富的物质基础

有利的沉积相带不仅可为储层提供丰富的物质基础, 还可控制储层的分布。川东地区岩溶储层主要分布在茅二、茅三段, 而颗粒滩相(包括台内滩与台缘滩)也主要分布在茅二、茅三段(图 8a—图 8c), 根据研究区 112 口井茅口组颗粒滩累计厚度和测井解释储层累计厚度统计发现, 颗粒滩厚度与储层厚

度呈明显正相关关系(图 9)。其中, SF 1 井滩体厚度最大, 累计达 94 m, 储层累计厚度达 35 m; F 1 井滩体厚度最小, 累计为 3 m, 储层累计厚度 2 m。颗粒灰岩厚度等值线与岩溶储层厚度等值线也具有较好的耦合关系(图 8)。

颗粒滩通常位于古地貌隆起区, 具有较高的水动力条件。海平面轻微下降会导致颗粒滩暴露, 进而经历大气淡水淋滤和溶蚀过程, 促进粒间溶孔与粒内溶孔发育^[25-26], 并且孔洞的发育与岩石颗粒大小有明显的关系。研究区颗粒滩相中主要发育生屑颗粒灰岩与藻屑颗粒灰岩, 岩石颗粒结构较粗, 且处于浅埋藏期的颗粒灰岩尚未胶结完全, 保留较多的原生孔隙, 为后期岩溶水提供渗滤通道, 加速岩溶作用发生, 在组构选择性孔隙的基础上继续溶扩而形成溶扩缝、溶蚀孔洞甚至洞穴, 从而促进岩溶储层的形成。

4.2 岩溶古地貌控制着岩溶储层的分布

前人研究认为, 除颗粒滩外岩溶古地貌对岩溶储层的发育分布也有显著影响, 且不同古地貌单元导致储层分布的差异^[27]。结合前人的划分依据, 本次研究在张亚等(2020 年)对茅口组顶部的岩溶古地貌的恢复的基础上^[28], 进一步细化三级岩溶古地貌。

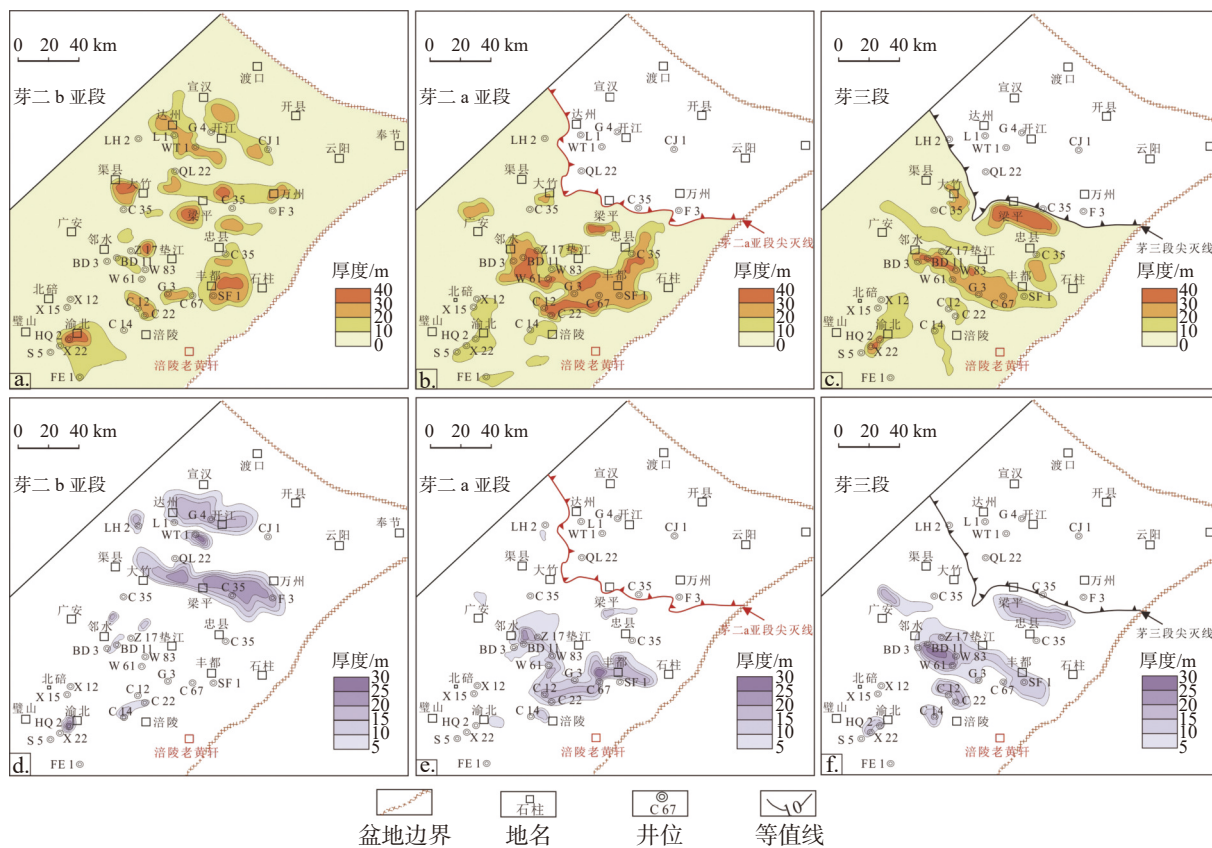


图8 川东地区茅口组颗粒灰岩厚度与岩溶储层厚度等值线图

a-c.茅二 b 亚段—茅三段颗粒灰岩厚度等值线图 d-f.茅二 b 亚段—茅三段岩溶储层厚度等值线图

Fig. 8 Isopleth map of granular limestone thickness and karst reservoir thickness in the Maokou Formation of the eastern Sichuan basin

(a-c. Mao Erb sub section~Mao San section granular limestone thickness contour map. d-f. Contour map of karst reservoir thickness from Mao-2b sub section to Mao-3 section)

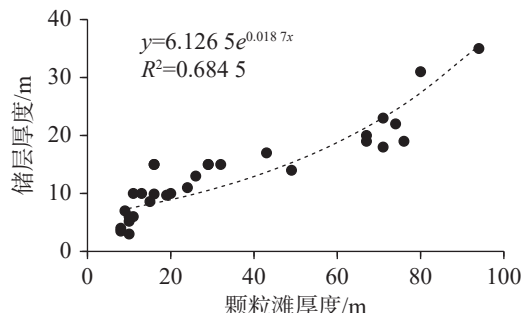


图9 川东地区中二叠统茅口组颗粒滩厚度与储层厚度相关图

Fig. 9 Correlation diagram of grain shoal thickness and reservoir thickness of the Middle Permian Maokou Formation in the eastern Sichuan region

将其划分为岩溶高地、岩溶陡坡、岩溶缓坡与岩溶盆地4个二级地貌单元, 岩溶高地、岩溶陡坡与岩溶缓坡内发育残丘与浅洼等三级地貌单元。

根据研究区岩溶古地貌单元与单井日产气量、岩溶储层分布叠合图可见(图10), 高产井主要分布

在研究区的岩溶陡坡地带, 如BD 3井与X 15井日产量分别为 $83.2 \times 10^4 \text{ m}^3$ 、 $112.83 \times 10^4 \text{ m}^3$, 岩溶高地与岩溶陡坡的过渡区次之。岩溶缓坡中残丘区域也发育产气井, 但产量大多低于岩溶陡坡和高地, 岩溶盆地中则没有发现茅口组产气井。这说明, 在颗粒滩的基础上, 岩溶储层的分布也受岩溶古地貌的影响。

岩溶高地主要分布在研究区南部, 古地貌地势高部。岩溶高地风化淋滤作用较为显著, 其不整合面附近的残余地层主要为茅四段。地表水系不发育, 以大气降水为主, 大气淡水以垂向渗流或片流的形式汇聚至地表以下, 岩溶高地地势较陡, 汇水范围小, 主要发生垂直渗流侵蚀。且渗流带溶蚀的物质不能快速被带走, 使形成的溶蚀缝洞被充填, 仅在残丘中保留较好的高角度裂缝和溶洞, 但连通性较差, 裂缝发育区可大大改善储层质量。

岩溶陡坡主要分布在岩溶高地的四周, 分布范围大, 地势较岩溶高地低。地形变化和水系汇合扩

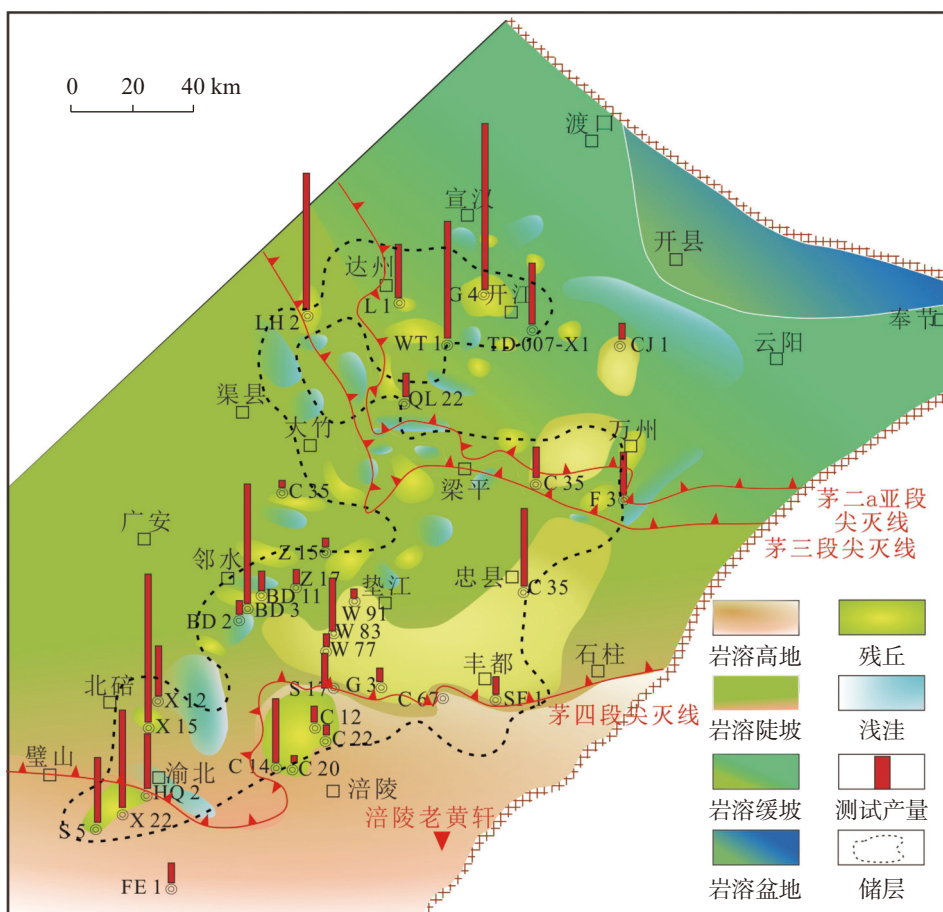


图 10 川东地区茅口组岩溶古地貌单元与单井日产气量、岩溶储层分布叠合图(据文献 [28] 改)

Fig. 10 Composite map of karst paleogeomorphological units, daily gas production of single well, and karst reservoir distribution in the Maokou Formation of the eastern Sichuan region (modified according to reference [28])

大了侵蚀区域,剥蚀作用强于岩溶高地,有利于岩溶储层的形成。岩溶水从高地向陡坡流动,该地貌单元以垂直渗流为主,水平径流相对较少。且受地貌与坡度的影响,溶蚀物质可快速被带走,因此岩溶陡坡中储集层主要发育垂向溶孔和高角度溶蚀缝,在残丘中发育未被充填的大型溶洞。

岩溶缓坡坡度比岩溶陡坡小,岩溶水以水平径流为主,在地势高部可见垂向渗流。但因地形封闭,岩溶作用时间延长,溶蚀作用的物质不易被带走,使先前形成的溶蚀孔洞又被后期岩溶水所携带物质充填,不利于孔洞的保存。岩溶储层在浅洼等单元发育较差。

综上所述,岩溶高地与岩溶陡坡的过渡区、岩溶陡坡与岩溶缓坡中的残丘地貌单元是茅口组岩溶储层发育的优势地区。

4.3 多期裂缝有利于形成岩溶缝洞储层

地下裂缝的类型多样,研究区茅口组沉积后共

遭遇四次大规模构造抬升运动——东吴运动、印支运动、燕山运动与喜山运动,产生了三期裂缝,分别为早期缝、中期缝和晚期缝^[29]。早期缝是在二叠系沉积过程中,包括茅口组遭受剥蚀时期由东吴运动所形成,因当时的上覆岩层较薄,使垂向应力为最小主应力,故基本为高角度缝或垂直缝,且多被全充填(图 11a);中期缝是印支运动和燕山运动所形成,因当时二叠系之上已沉积多套地层,使垂向应力为最大主应力,故基本为高角度斜交缝或 X 形剪切缝,且多被全充填或半充填(图 11b);晚期缝应是由喜山运动所形成,因该次运动十分强烈,基本形成了四川盆地的构造格局,故水平构造应力为最大主应力,而垂向应力为中间主应力,故基本为水平裂缝,且充填程度较低,甚至无充填(图 11c)。通过对研究区岩心的观察发现,缝洞型岩溶储层裂缝与孔洞既有分离状态,又有串珠状态,说明茅口组早期缝在茅口组遭受剥蚀之后形成,且在裂缝形成后古岩溶仍再继续,而

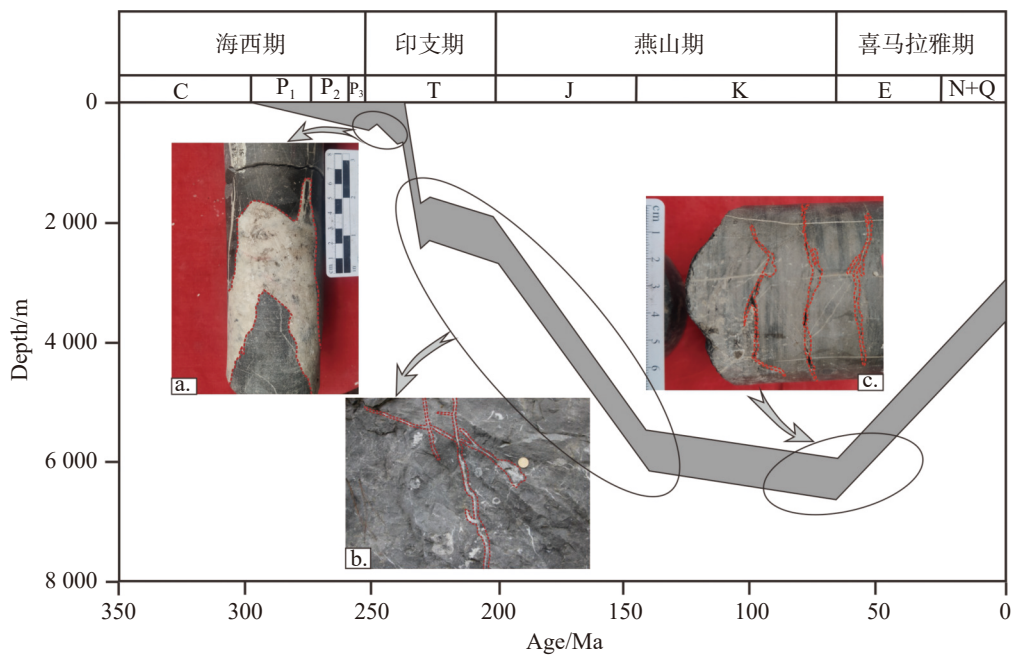


图 11 C 7 井埋藏史图与裂缝期次叠合图(据文献 [30] 改)

a.高角度早期缝 b.全平填X剪切中期缝 c.水平张开晚期缝

Fig. 11 Burial history of Well C7 and superimposition of fracture generation (modified according to reference [30])

a. High angle early seam b. Fully filled X shear mid-term seam c. Horizontal opening late stage seam

晚期缝与古岩溶孔洞基本呈分离状态,但晚期缝不仅可与早期缝相切割而沟通古岩溶孔洞,还可能在剖面中沟通看似独立的储层而构成大的储渗系统,以大幅度提高产量。如位于研究区北部卧龙河构造的W 78井,其茅二a亚段岩心裂缝密度达 $11\text{条}\cdot\text{m}^{-1}$,并形成丰富的岩溶缝洞、岩溶裂缝以及岩溶孔隙型储层。当不同期次的规模发育裂缝带相互切割时,溶蚀与冲蚀作用在该处易于发生,形成规模较大的岩溶储层。

5 有利勘探区带优选

充足的物质来源、有利的成岩作用与构造运动是形成优质储层的基础。通过上述对于茅口组岩溶储层主控因素的分析,优选出两个有利区:邻水—丰都一带以及达州—开江一带。由图10可知,邻水—丰都一带茅四段已被剥蚀殆尽,处于岩溶陡坡单元中,在茅二a亚段与茅三段广泛发育颗粒滩(图8b,图8c),已有钻井显示,该区域残丘三级地貌单元中岩溶作用强烈,储层物性较好,因此具有较好的油气产量,而浅洼中,岩溶作用较弱,溶蚀孔洞易被快速充填降低储层的物性,油气产量较低。达州—开江一带茅口组已被剥蚀至茅二b亚段,虽处于岩溶缓

坡中,岩溶作用较弱,但该地区多期裂缝叠置发育^[26],促进了储层渗滤能力,也具有较高的油气产量。综上所述,研究区邻水—丰都一带与达州—开江一带分别处于岩溶陡坡与岩溶缓坡中,其残丘地貌发育区为预测有利岩溶储层区。

6 结 论

(1)基于野外、钻井和地震资料,总结了研究区茅口组岩溶储层识别特征。岩石学方面:岩心与露头常具有残余溶蚀孔洞与裂缝,地层顶部可见铝土质黏土岩及含褐铁矿的岩溶角砾;测井方面:自然伽玛小于40API、三孔隙度与双侧向电阻率曲线呈现箱型、成像测井表现为黑色斑块状;录井方面:见井漏与放空;地震剖面:呈现出“低频、强振幅、宽波峰”特征,当缝洞较多时,还会出现“亮点”反射特征。

(2)岩溶储层中主要储集岩为颗粒灰岩,主要储集空间为溶孔、溶洞;岩溶储层物性表现为低孔低渗的特征,孔洞型储层物性最佳;岩溶储层纵向上主要分布在距茅口组顶部100 m范围内,以孔洞型储层最为发育,横向分布延展性较差,平面上在邻水—丰都一带呈北西—南东向的带状分布。

(3)颗粒滩厚度与岩溶储层厚度呈明显的正相

关系,说明颗粒滩为岩溶储层优质的物质基础,并且可为后期成岩流体提供渗滤通道;高产井大多分布在岩溶高地与岩溶陡坡的过渡区和残丘地貌单元中,说明岩溶古地貌控制了岩溶储层的分布;多期裂缝改善了储层的储集性能,并为油气渗滤提供通道,促进大型油气藏的聚集。

参考文献

- [1] 张宇,赵伦,李长海,张祥忠.古岩溶油气储层研究进展[J].*中国岩溶*,2022,41(5):808-824.
ZHANG Yu, ZHAO Lun, LI Changhai, ZHANG Xiangzhong. Research progress of paleokarst oil and gas reservoirs[J]. *Carso-logic Sinica*, 2022, 41(5): 808-824.
- [2] 马永生,何登发,蔡勋育,刘波.中国海相碳酸盐岩的分布及油气地质基础问题[J].*岩石学报*,2017,33(4):1007-1020.
MA Yongsheng, HE Dengfa, CAI Xunyu, LIU Bo. Distribution and fundamental science questions for petroleum geology of marine carbonate in China[J]. *Acta Petrologica Sinica*, 2017, 33(4): 1007-1020.
- [3] Hollis, C. Diagenetic controls on reservoir properties of carbonate successions within the Albian-Turonian of the Arabian Plate. *Petrol. Geo-sci.* 2011, 17(3), 223-241.
- [4] HAO Yuxin , Rebecca Bell, HU Dongfeng, FAN Rui, WANG Yanghua. WITHDRAWN: Prediction of Permian karst reservoirs in the Yuanba gas field, northern Sichuan Basin, China[J]. *Marine and Petroleum Geology*, 2023, 154: 106160.
- [5] 张玺华,田兴旺,杨岱林,王云龙,孙奕婷,洪海涛,夏茂龙,汪华,徐亮.四川盆地海相碳酸盐岩储层成因及特征[J].*天然气勘探与开发*,2021,44(3):1-10.
ZHANG Xihua, TIAN Xinwang, YANG Dailin, WANG Yunlong, SUN Yiting, HONG Haitao, XIA Maolong, WANG Hua, XU Liang. Genesis and characteristics of marine carbonate reservoirs in Sichuan Basin[J]. *Natural Gas Exploration and Development*, 2021, 44(3): 1-10.
- [6] 江青春,胡素云,汪泽成,池英柳,杨雨,鲁卫华,王海真,李秋芬.四川盆地茅口组风化壳岩溶古地貌及勘探选区[J].*石油学报*,2012,33(6):949-960.
JIANG Qingchun, HU Shuyun, WANG Zecheng, CHI Yingliu, YANG Yu, LU Weihua, WANG Haizhen, LI Qiufen. Paleokarst landform of the weathering crust of Middle Permian Maokou Formation in Sichuan Basin and selection of exploration regions[J]. *Acta Petrolei Sinica*, 2012, 33(6): 949-960.
- [7] 李素华,胡昊,朱兰,余洋,石国山,贾霍甫.川北元坝地区茅口组生屑滩岩溶储层识别及预测[J].*石油物探*,2021,60(4):584-594.
LI Suhua, HU Hao, ZHU Lan, YU Yang, SHI Guoshan, JIA Huofu. Identification of bioclastic beach reservoir in Maokou formation, Yuanba area, north Sichuan Basin[J]. *Geophysical Prospecting for Petroleum*, 2021, 60(4): 584-594.
- [8] 戴晓峰,冯周,王锦芳.川中茅口组岩溶储层地球物理特征及勘探潜力[J].*石油地球物理勘探*,2017,52(5):1049-1058,882.
DAI Xiaofeng, FENG Zhou, WANG Jinfang. Geologic and geo-physical characteristics and exploration potential of karst reservoirs at Maokou Formation in the central Sichuan Basin[J]. *Oil Geophysical Prospecting*, 2017, 52(5): 1049-1058, 882.
- [9] 冯磊,刘宏,谭磊,夏吉文,伍亚,陈聪,曾云贤,于童.岩溶古地貌恢复及油气地质意义:以四川盆地泸州地区中二叠统茅口组为例[J].*断块油气田*,2023,30(1):60-69.
FENG Lei, LIU Hong, TAN Lei, XIA Jiwen, WU Ya, CHEN Cong, ZENG Yunxian, YU Tong. Karst paleogeomorphology restoration and hydrocarbon geological significance: a case study of middle Permian Maokou Formation in Luzhou area of Sichuan Basin[J]. *Fault-Block Oil & Gas Field*, 2023, 30(1): 60-69.
- [10] 杨明磊,诸丹诚,李涛,李海平,黎霆,邹华耀.川南地区中二叠统茅口组颗粒滩对早成岩期岩溶储层的控制[J].*现代地质*,2020,34(2):356-369.
YANG Minglei, ZHU Dancheng, LI Tao, LI Haiping, LI Ting, ZOU Huayao. Control of eogenetic karst reservoir by shoals in Middle Permian Maokou Formation, southern Sichuan Basin[J]. *Geoscience*, 2020, 34(2): 356-369.
- [11] 王国锋,张大伟,邓守伟,杨光,宋文礼.四川盆地自贡区块茅口组岩溶储层发育特征及其主控因素[J].*天然气工业*,2022,42(9):63-75.
WANG Guofeng, ZHANG Dawei, DENG Shouwei, YANG Guang, SONG Wenli. Development characteristics and main controlling factors of Maokou Formation karst reservoirs in Zigong block of the Sichuan Basin[J]. *Natural Gas Industry*, 2022, 42(9): 63-75.
- [12] 曹华,陈延贵,陈聪,高兆龙,山述娇,李天军,胡罗嘉,谢静平.四川盆地东北部茅口组岩溶储层控制因素[J].*天然气勘探与开发*,2022,45(3):1-10.
CAO Hua, CHEN Yanqiu, CHEN Cong, GAO Zhao long, SHAN Shujiao, LI Tianjun, HU Luojia, XIE Jingping. Controlling factors of karst reservoir in Maokou Formation, northeastern Sichuan Basin[J]. *Natural Gas Exploration and Development*, 2022, 45(3): 1-10.
- [13] 何斌,徐义刚,王雅政,肖龙.东吴运动性质的厘定及其时空演变规律[J].*地球科学(中国地质大学学报)*,2005,30(1):89-96.
HE Bin, XU Yigang, WANG Yamei, XIAO Long. Nature of the Dongwu movement and its temporal and spatial evolution[J]. *Earth Science(Journal of China University of Geosciences)*, 2005, 30(1): 89-96.
- [14] 黎荣,胡明毅,潘仁芳,胡忠贵.川中地区中二叠统断溶体发育特征及形成机制[J].*中国石油勘探*,2019,24(1):105-114.
LI Rong, HU Mingyi, PAN Renfang, HU Zhonggui. Development characteristics and forming mechanism of Middle Permian fault-karst carbonate reservoirs in the central Sichuan Basin[J]. *China Petroleum Exploration*, 2019, 24(1): 105-114.
- [15] 梁新权,周云,蒋英,温淑女,付建刚,王策.二叠纪东吴运动的沉积响应差异:来自扬子和华夏板块吴家坪组或龙潭组碎屑

- [15] 钙石 LA-ICPMS U-Pb 年龄研究 [J]. 岩石学报, 2013, 29(10): 3592-3606.
- LIANG Xinquan, ZHOUYUN, JIANG Ying, WEN Shunv, FU Jianguang, WANG Che. Difference of sedimentary response to Dongwu Movement: Study on LA-ICPMS U-Pb ages of detrital zircons from Upper Permian Wujiaping or Longtan Formation from the Yangtze and Cathaysia blocks[J]. Acta Petrologica Sinica, 2013, 29(10): 3592-3606.
- [16] 崔思华, 王明磊, 彭秀丽, 杨冬. 碳酸盐岩地层综合划分方法研究 [J]. 西南石油大学学报: 自然科学版, 2011, 33(5): 41-48.
- CUI Sihua, WANG Minglei, PENG Xiuli, YANG Dong. Study on the synthetical division method for carbonate formation [J]. Journal of Southwest Petroleum University: Science & Technology Edition, 2011, 33(5): 41-48.
- [17] 胡罗嘉, 黄世伟, 谭万仓, 谭秀成, 苏成鹏, 胡笙, 李明隆, 刘菲, 冯亮. 四川盆地东部二叠系茅口组层序地层特征及地质意义 [J]. 海相油气地质, 2021, 26(4): 357-366.
- HU Luojia, HUANG Shiwei, TAN Wanchang, TAN Xiucheng, SU Chengpeng, HU Sheng, LI Minglong, LIU Fei, FENG Liang. Sequence stratigraphic characteristics and geological significance of the Permian Maokou Formation in the eastern Sichuan Basin[J]. Marine Origin Petroleum Geology, 2021, 26(4): 357-366.
- [18] 罗鹏, 李国蓉, 施泽进, 周大志, 汤鸿伟, 张德明. 川东南地区茅口组层序地层及沉积相浅析 [J]. 岩性油气藏, 2010, 22(2): 74-78.
- LUO Peng, LI Guorong, SHI Zejin, ZHOU Dazhi, TANG Hongwei, ZHANG Deming. Analysis of sequence stratigraphy and sedimentary facies of Maokou Formation in southeastern Sichuan[J]. Lithologic Reservoirs, 2010, 22(2): 74-78.
- [19] 肖陈静, 胡修权, 施泽进, 谭谦, 李江寒, 易驰, 李世临, 徐发波. 利用滩地比技术描述碳酸盐岩沉积相: 以川东地区茅二 a 亚段为例 [J]. 中国岩溶, 2022, 41(6): 869-879.
- XIAO Jing, HU Xiuquan, SHI Zejin, TAN Qian, LI Jianghan, YI Chi, LI Shilin, XU Fabo. Describing carbonate sedimentary facies by use of the ratio of shoals to the whole strata: Taking the layer a of Mao2 submember in eastern Sichuan for example[J]. Garsologica Sinica, 2022, 41(6): 869-879.
- [20] 李红敬, 解习农, 颜佳新, 陈慧, 简晓玲. 扬子地区典型剖面二叠系不同沉积相地球化学特征 [J]. 地质科技情报, 2010, 29(2): 16-23.
- LI Hongjing, XIE Xinong, YAN Jiaxin, CHEN Hui, JIAN Xiaoling. Geochemical characteristics of different facies of Permian typical sections in the Yangtze region[J]. Geological and Technology Information, 2010, 29(2): 16-23.
- [21] 赵永刚, 陈景山, 李凌, 古永红, 张春雨, 张栋梁, 张文强, 周通. 基于残余岩溶强度表征和裂缝预测的碳酸盐岩储层评价: 统良里塔格组为例 [J]. 吉林大学学报: 地球科学版, 2015, 45(1): 25-36.
- ZHAO Yonggang, CHEN Jingshan, LI Ling, GU Yonghong, ZHANG Chunyu, ZHANG Dongliang, ZHANG Wenqiang, ZHOU Tong. Evaluation of carbonate reservoir based on residual karst intensity characterization and structural fracture predic-
- tion: A case from the Upper Ordovician Lianglitage Formation in the West of Center Tarim Basin[J]. Journal University: Earth Science Edition, 2015, 45(1): 25-36.
- [22] 李阳. 塔河油田奥陶系碳酸盐岩溶洞型储集体识别及定量表征 [J]. 中国石油大学学报(自然科学版), 2012, 36(1): 1-7.
- Li Yang. Ordovician carbonate fracture-cavity reservoirs identification and quantitative characterization in Tahe Oilfield[J]. Journal of China University of Petroleum (Natural Science Edition), 2012, 36(1): 1-7.
- [23] 程雪莹. 川东地区中二叠统茅口组岩溶特征及发育模式 [D]. 成都: 西南石油大学, 2017.
- Cheng X Y. Karst characteristics and development model of Maokou Formation of Middle Permian in eastern Sichuan Basin[D]. Chengdu: Southwest Petroleum University, 2017.
- [24] 桑琴, 黄静, 程超, 吴昌龙, 彭祚远. 蜀南地区茅口组古岩溶识别标志及储层预测 [J]. 大庆石油学院学报, 2012, 36(2): 53-57.
- SHANG Qin, HUANG Jing, CHENG Chao, WU Changlong, PENG Zhuoyuan. Identification mark and reservoir prediction of palaeokarst of the Maokou Formation in southern Sichuan Province[J]. Journal of Daqing Petroleum Institute, 2012, 36(2): 53-57.
- [25] 张满郎, 郭振华, 张林, 付晶, 郑国强, 谢武仁, 马石玉. 四川安岳气田龙王庙组颗粒滩岩溶储层发育特征及主控因素 [J]. 地学前缘, 2021, 28(1): 235-248.
- ZHANG Manlang, GUO Zhenhua, ZHANG Lin, FU Jing, ZHENG Guoqiang, XIE Wuren, MA Shiyu. Characteristics of and main factors controlling the karst shoal reservoir of the Lower Cambrian Longwangmiao Formation in the Anyue gas field, central Sichuan Basin, China[J]. Earth Science Frontiers, 2021, 28(1): 235-248.
- [26] 李珊珊, 姜鹏飞, 刘磊, 雷程, 曾云贤, 陈仕臻, 周刚. 四川盆地高磨地区寒武系沧浪铺组碳酸盐岩颗粒滩地震响应特征及分布规律 [J]. 岩性油气藏, 2022, 34(4): 22-31.
- LI Shanshan, JIANG Pengfei, LIU Lei, LEI Cheng, ZENG Yunxian, CHEN Shizhen, ZHOU Gang. Seismic response characteristics and distribution law of carbonate shoals of Cambrian Canglangpu Formation in Gaoshiti-Moxi area, Sichuan Basin[J]. Lithologic Reservoirs, 2022, 34(4): 22-31.
- [27] 肖笛, 谭秀成, 山述娇, 陈韵骐, 夏吉文, 杨坚, 周涛, 程遥. 四川盆地南部中二叠统茅口组古岩溶地貌恢复及其石油地质意义 [J]. 地质学报, 2014, 88(10): 1992-2002.
- XIAO Di, TAN Xiucheng, SHAN Shujiao, CHEN Yunqi, XIA Jiwen, YANG Jian, ZHOU Tao, CHENG Yao. The restoration of palaeokarst geomorphology of Middle Permian Maokou Formation and its petroleum geological significance in southern Sichuan Basin[J]. Acta Geologica Sinica, 2014, 88(10): 1992-2002.
- [28] 张亚, 陈双玲, 张晓丽, 张玺华, 谢忱, 陈聪, 杨雨然, 高兆龙. 四川盆地茅口组岩溶古地貌刻画及油气勘探意义 [J]. 岩性油气藏, 2020, 32(3): 44-55.
- ZHANG Ya, CHEN Shuangling, ZHANG Xiaoli, ZHANG Xihua, XIE Chen, CHEN Cong, YANG Yuran, GAO Zhaolong.

- Restoration of paleokarst geomorphology of Lower Permian Maokou Formation and its petroleum exploration implication in Sichuan Basin. *Lithologic Reservoirs*, 2020, 32(3): 44-55.
- [29] 马珂欣, 胡明毅, 史今雄, 邓庆杰. 川西南自贡地区二叠系茅口组储层裂缝特征及期次演化[J]. 地质科技通报, 2024, 43(3): 180-191.
MA Kexin, HU Mingyi, SHI Jinxiong, DENG Qingjie. Characteristic and formation period of fractures in the reservoirs of Per-
- [30] mian Maokou Formation, Zigong area, Southwest Sichuan Basin[J]. *Journal University: Earth Science Edition*, 2024, 43(3): 180-191.
TANG Xianglu, JIANG Zhenxue, JIANG Shu, WANG Hongyan, HE Zhiliang, FENG Jie. Structure, burial, and gas accumulation mechanisms of lower Silurian Longmaxi Formation shale gas reservoirs in the Sichuan Basin (China) and its periphery[J]. *AAPG Bulletin*, 2021, 105(12): 2425-2447.

Characteristics and dominant controlling factors of karst reservoirs in the middle Permian Maokou Formation of the eastern Sichuan region

YANG Rong¹, YANG Xiyan¹, FAN Cunhui¹, LI Yang¹, LI Yue², HUANG Zisang³

(1. School of Geoscience and Technology, Southwest Petroleum University, Chengdu, Sichuan 610500, China; 2. Exploration and Development Research Institute of PetroChina Southwest Oil and Gas Field Company, Chengdu, Sichuan 610041, China;
3. Chengdu University of Technology, Chengdu, Sichuan 610059, China)

Abstract The middle Permian Maokou Formation in the eastern Sichuan region is characterized by the widespread development of karst reservoirs. However, systematic analysis of the identification criteria and controlling factors of these karst reservoirs remains insufficient. This study integrates extensive field outcrops, drilling cores, thin sections, well logging and well logging interpretation, and seismic data to comprehensively analyze the response characteristics of karst reservoirs in the Maokou Formation of the eastern Sichuan region. Furthermore, this paper elucidates the fundamental characteristics and distribution patterns of these reservoirs while conducting a comprehensive evaluation of their primary controlling factors. The key findings are as follows.

(1) Karst reservoirs exhibit a variety of identification markers. The petrological response characteristics are as follows: residual dissolution pores, ranging from 2 mm to 70 mm in diameter, and fractures—mainly high-angle structural fractures—are generally developed in both cores and outcrops. Additionally, the caves are mostly half-filled with calcite, dolomite, or asphalt, while some remain unfilled. Bauxitic clay rocks and karst breccia containing limonite are visible at the top of the stratum, indicating the existence of ancient weathering crust. The logging response characteristics are as follows, the acoustic time difference, compensated neutron curves and compensated density curves are "box-shaped" in the karst cave section. The phenomena of pronounced acoustic time difference leap are observed, accompanied by a reduction in the positive difference of deep and shallow dual lateral resistivity. Imaging logging shows the black patchy karst cave characterized by low resistance and high conductivity. Natural gamma values in the karst cave section is generally lower than 40 API, with low content of radioactive elements. The logging response is characterized by frequent well leakage and venting during drilling, mainly occurring in the range of 0 m to 100 m from the top of the Maokou Formation. High-yield gas wells are mostly located in the second and third members of the Maokou Formation, reflecting the development of fracture-cavity reservoirs. The seismic response characteristics are marked by "low-frequency, high-amplitude, and wide-crest" reflections at the top of the Maokou Formation. In the dense area of karst caves, "bright spots" anomalies appear. The development of karst caves reduces wave impedance difference, resulting in downward-dragged and chaotic reflections.

(2) The rocks of karst reservoirs are mainly composed of grain limestone. The main reservoir spaces consist of dissolved pores and caves, with caves being the most significant reservoir space, accounting for more than 65 %. These caves are predominantly distributed in isolated patterns, exhibiting poor connectivity. Dissolved pores, including intragranular, intergranular, and intercrystal types are predominantly filled. The measured porosity of the karst reservoir ranges from 2.0% to 8.7 %, with an average of 3.4 %. The permeability varies from 0.008 mD to 65.263 mD,

averaging 18.3 mD, showing the characteristics of low porosity and low permeability. Among the three types of karst reservoirs, fracture-cavity reservoirs exhibit the most favorable physical properties, with a porosity of 3.3 %, and a permeability of 23.3 mD. In contrast, the cavity-type reservoirs demonstrate inferior physical properties due to the lack of filtration channels. Karst landforms are categorized into karst highlands, steep karst slopes, gentle karst slopes, and karst basins. The porosity of steep karst slopes (3.96 %) is significantly higher than that of gentle karst slopes (3.27 %) and karst highlands (2.10%). Vertically, the karst reservoirs are mainly distributed within 100 m from the top of the Maokou Formation, particularly in the Mao 2a sub-member and the Mao 3 member. These reservoirs exhibit poor lateral ductility, presenting as isolated point-like or belt-like distributions. Horizontally, there is a NW–SE zonal distribution in the Linshui–Fengdu area, with reservoir thicknesses ranging from 7.68 m to 11.04 m.

(3) Karst reservoirs are influenced by the combined effects of sedimentation, karstification and tectonism. Specifically, the grain shoals (intra-platform shoals and platform margin shoals) are mainly developed in the Mao 2 and the Mao 3 members. The thickness of the granular limestone is positively correlated with the thickness of the reservoir ($R^2 = 0.82$), which indicates that the grain shoals provide a high-quality material foundation for the karst reservoirs and offer percolation channels for diagenetic fluids in later stages. The karst paleogeomorphology controls the distribution of karst reservoirs. High-yield wells are mostly located in the geomorphic units of residual mounds on steep karst slopes and gentle karst slopes. The transitional zones between karst highlands and karst steep karst slopes are also favorable areas for the development of karst reservoirs. Multiple stages of fracturing improve the reservoir storage performance. Specially, three stages of fractures came into being during the Dongwu Movement (early high-angle fractures), the Indosinian–Yanshan Movement (mid-term X-shaped fractures), and the Himalayan Movement (late horizontal fractures). The late horizontal fractures intersected the earlier fractures and connected with karst caves, significantly enhancing the permeability. For instance, the fracture density of Well W78 reached 11 fractures/m, resulting in a substantial increase in daily gas production. These fractures provide channels for oil and gas infiltration, facilitating the accumulation of large oil and gas reservoirs.

(4) Based on the analysis of the dominant controlling factors, two favorable areas have been identified. The first is the Linshui–Fengdu steep karst slope zone, which is characterized by thick grain shoals reaching up to 23 m in the Mao 3 Member, the well-developed residual mound landform, dense karst caves and fractures, all of which contribute to optimal reservoir physical properties. The second is the Dazhou–Kaijiang gentle karst slope zone. This zone features the superposition of multi-stage fractures, particularly mid-term fractures, which significantly enhance permeability. Although karstification is relatively weak, this area has the potential of high-yield production.

Key words karst reservoir, reservoir characteristics, dominant controlling factor, the Maokou Formation, the eastern Sichuan region

(编辑 张玲)